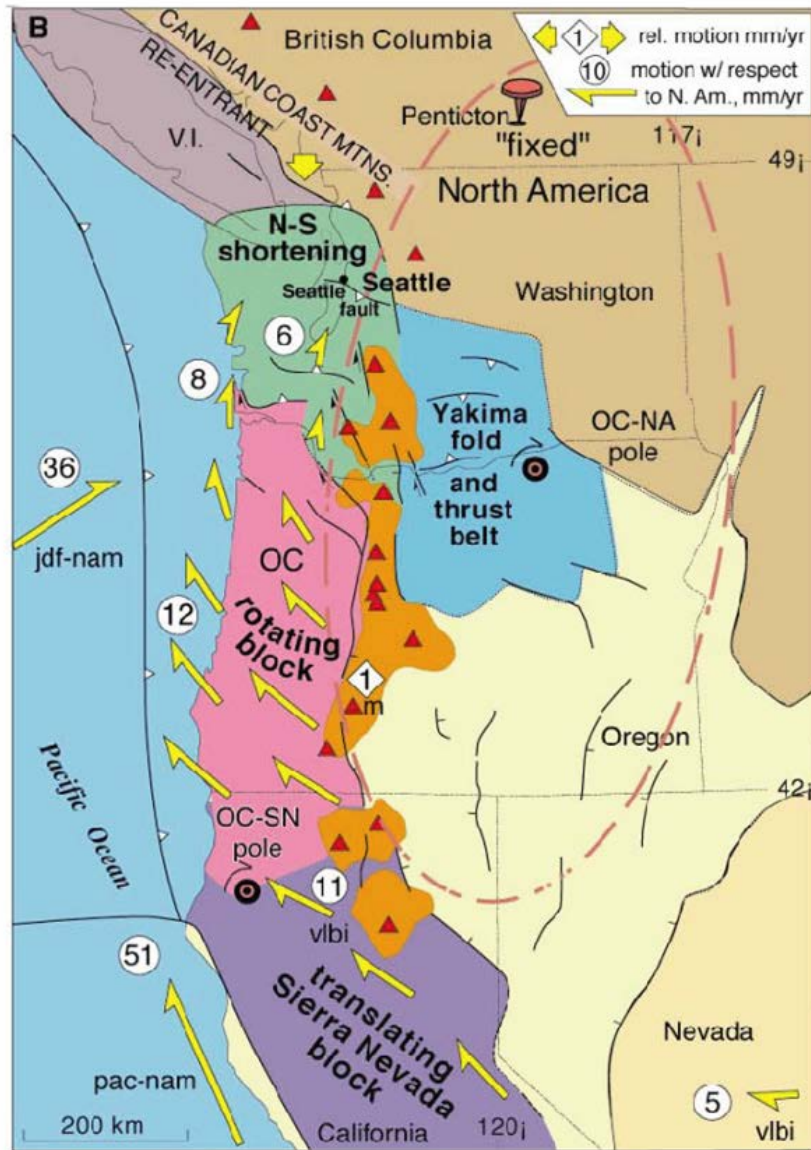


Mass Fluxes and Deformation in the Cascadia Subduction Wedge

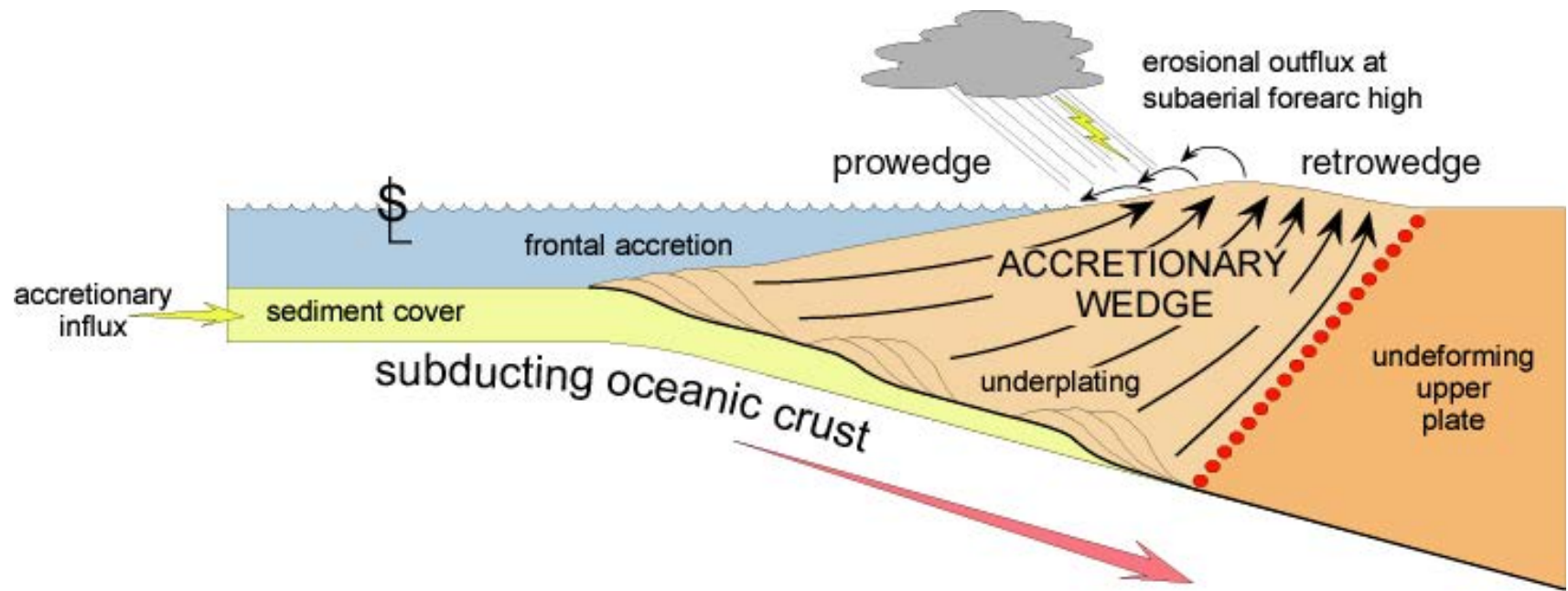
Mark Brandon,
Yale University



RIGID BLOCKS:

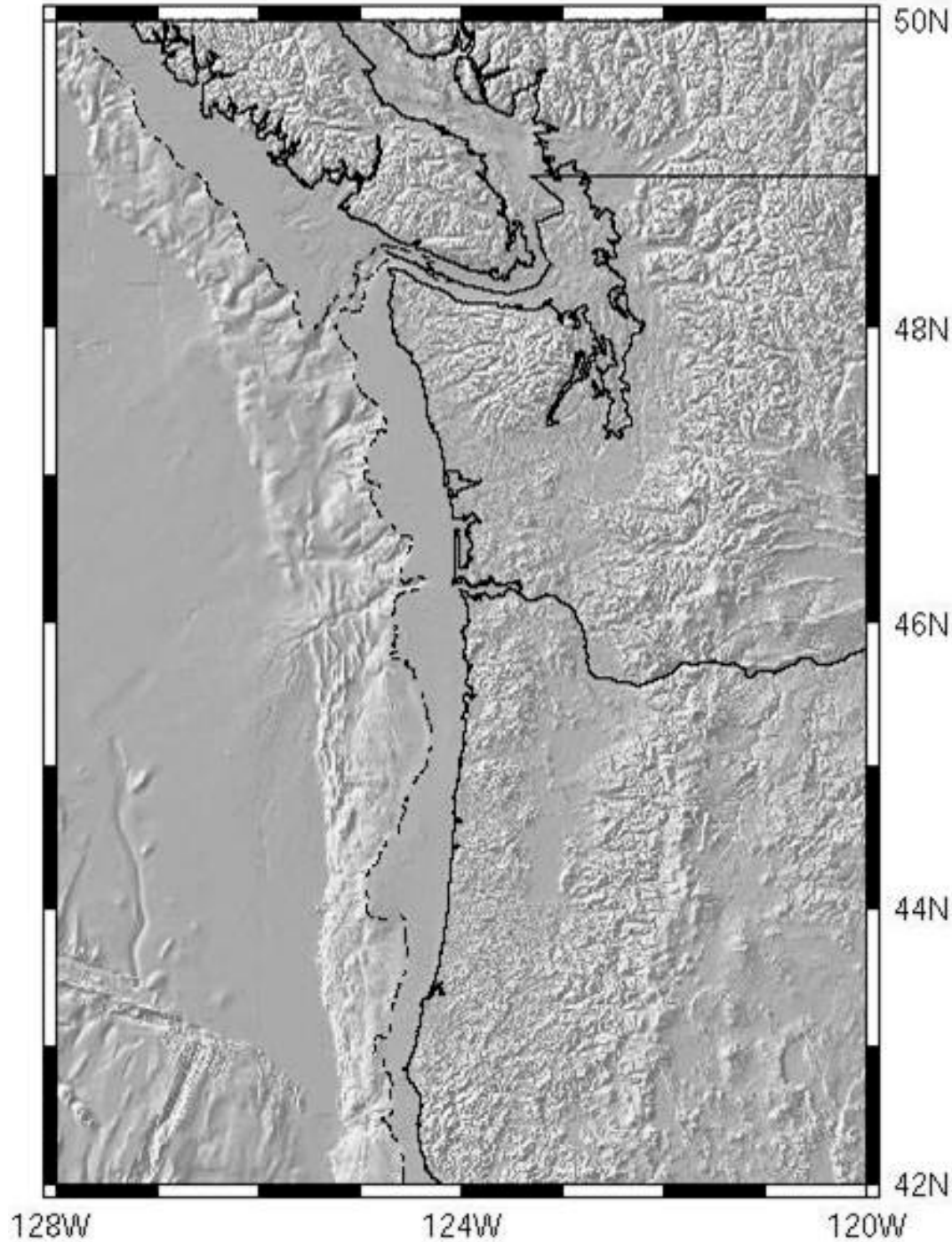
Collision of Oregon block with Vancouver Island buttress (e.g., Walcott, 1993; Wang, 1996; Wells et al., 1998; MacCaffrey et al., 2000) .

Prediction: large E-W trending uplift and average N-S horizontal strain rate of ~ 35 nanostrain yr^{-1} . (assumes north velocity of 6 to 8 mm/yr accommodated by shortening over a ~ 200 km length scale.)



WIDE WEDGE: Accretion drives deformation in a subduction wedge that extends beneath the Coast Ranges (Brandon et al., 1998; Pazzaglia and Brandon, 2001; Batt et al., 2001).

Prediction: NE-SW shortening in the direction of plate convergence. Current estimates for the Olympics Mountains indicate NE-SW shortening across the uplift related to a velocity change of ~ 4 mm/yr distributed over 120 km length scale, which is equal to an average of ~ 33 nanostrain/yr.



Shelf is undeformed, which precludes significant N-S shortening across the Olympics

Figure: Brandon, 2004



Los Angeles

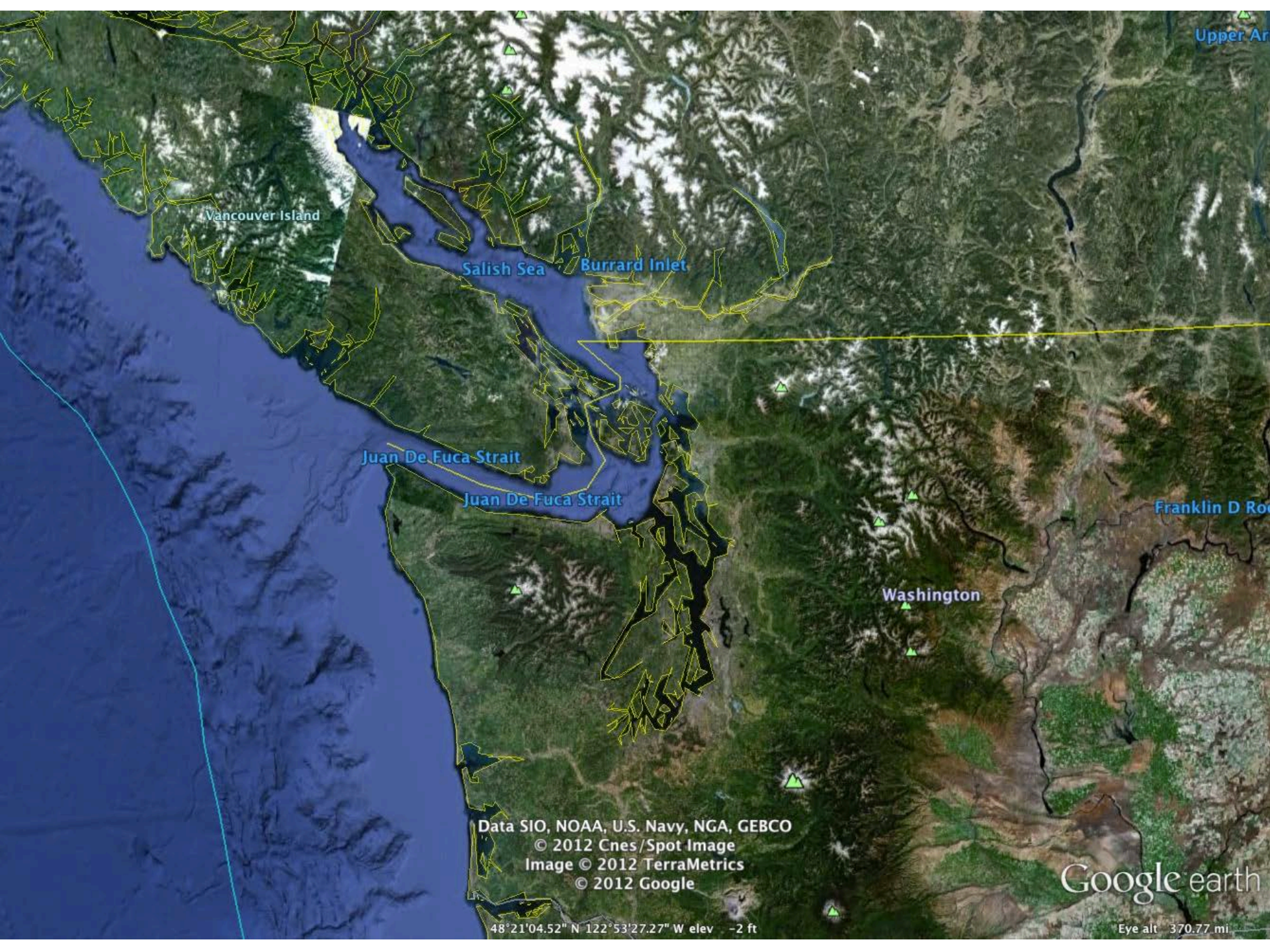
San Diego

Data SIO, NOAA, U.S. Navy, NGA, GEBCO
© 2012 INEGI
Image © 2012 TerraMetrics
© 2012 Google

Google earth

33°41'14.04" N 118°12'05.18" W elev 0 ft

Eye alt 424.11 mi



Vancouver Island

Salish Sea

Burrard Inlet

Juan De Fuca Strait

Juan De Fuca Strait

Washington

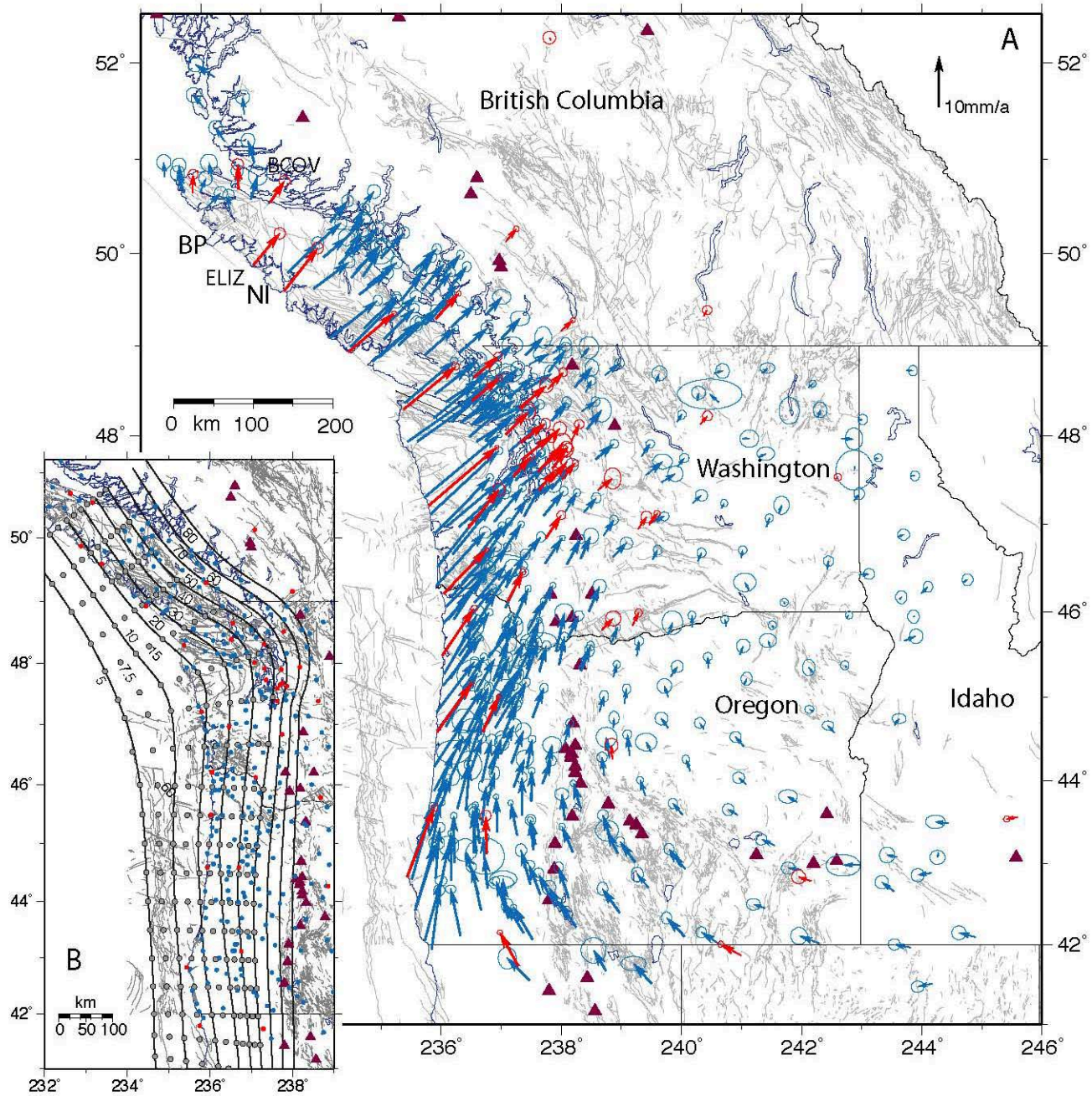
Franklin D Roosevelt

Data SIO, NOAA, U.S. Navy, NGA, GEBCO
© 2012 Cnes/Spot Image
Image © 2012 TerraMetrics
© 2012 Google

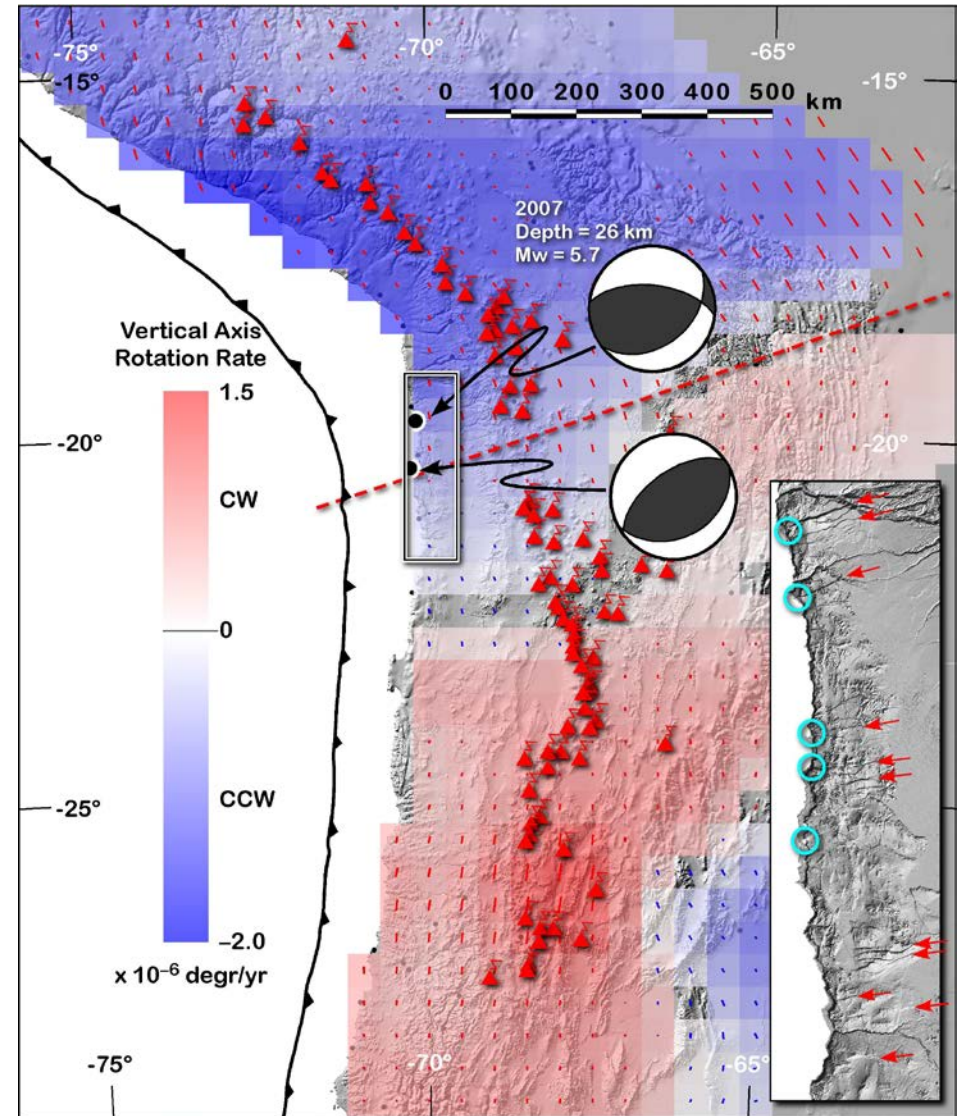
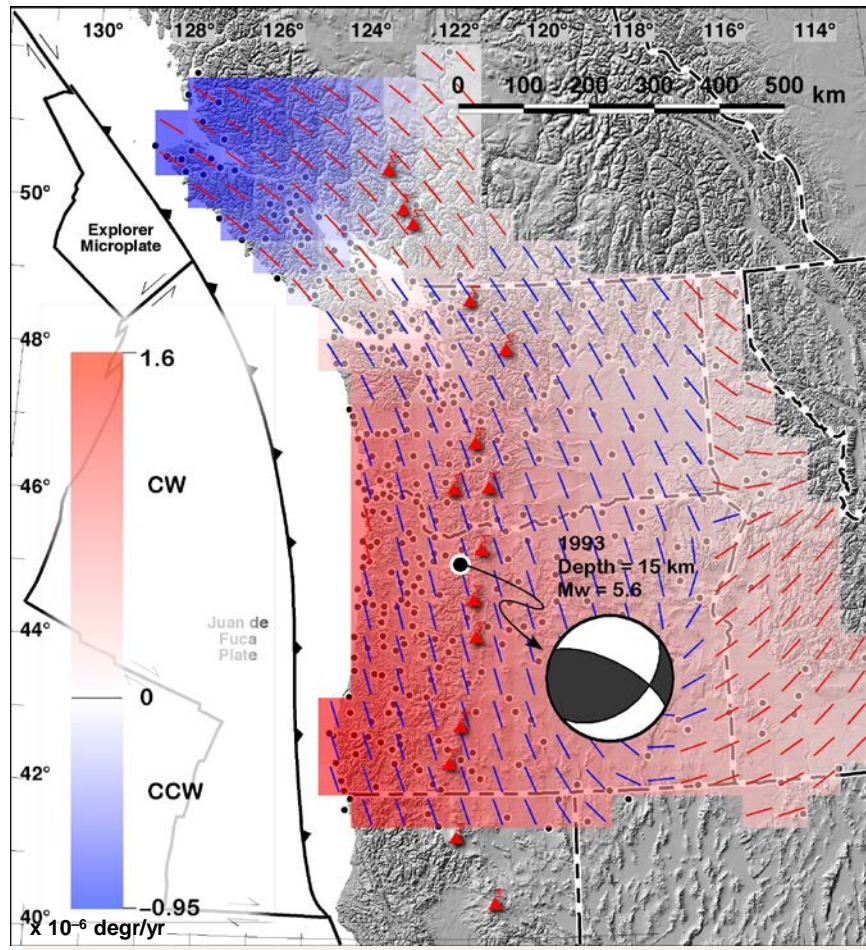
Google earth

48°21'04.52" N 122°53'27.27" W elev -2 ft

Eye alt 370.77 mi

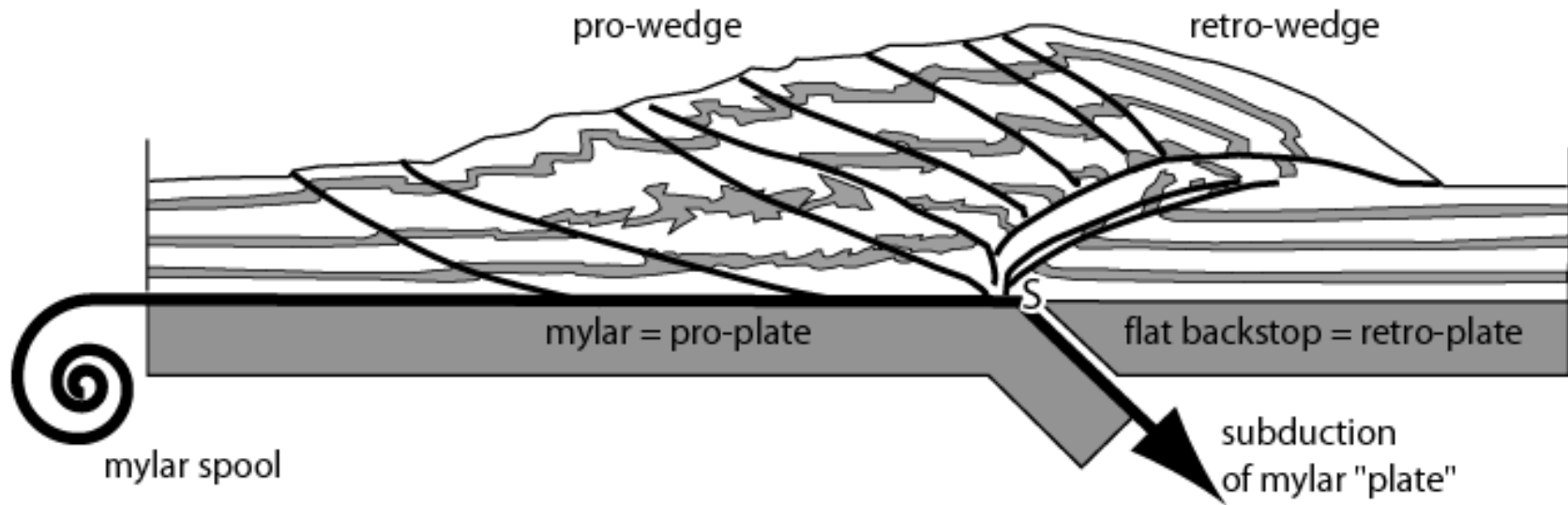


Vertical Axis Rotations for Cascadia and Chile Geodetics



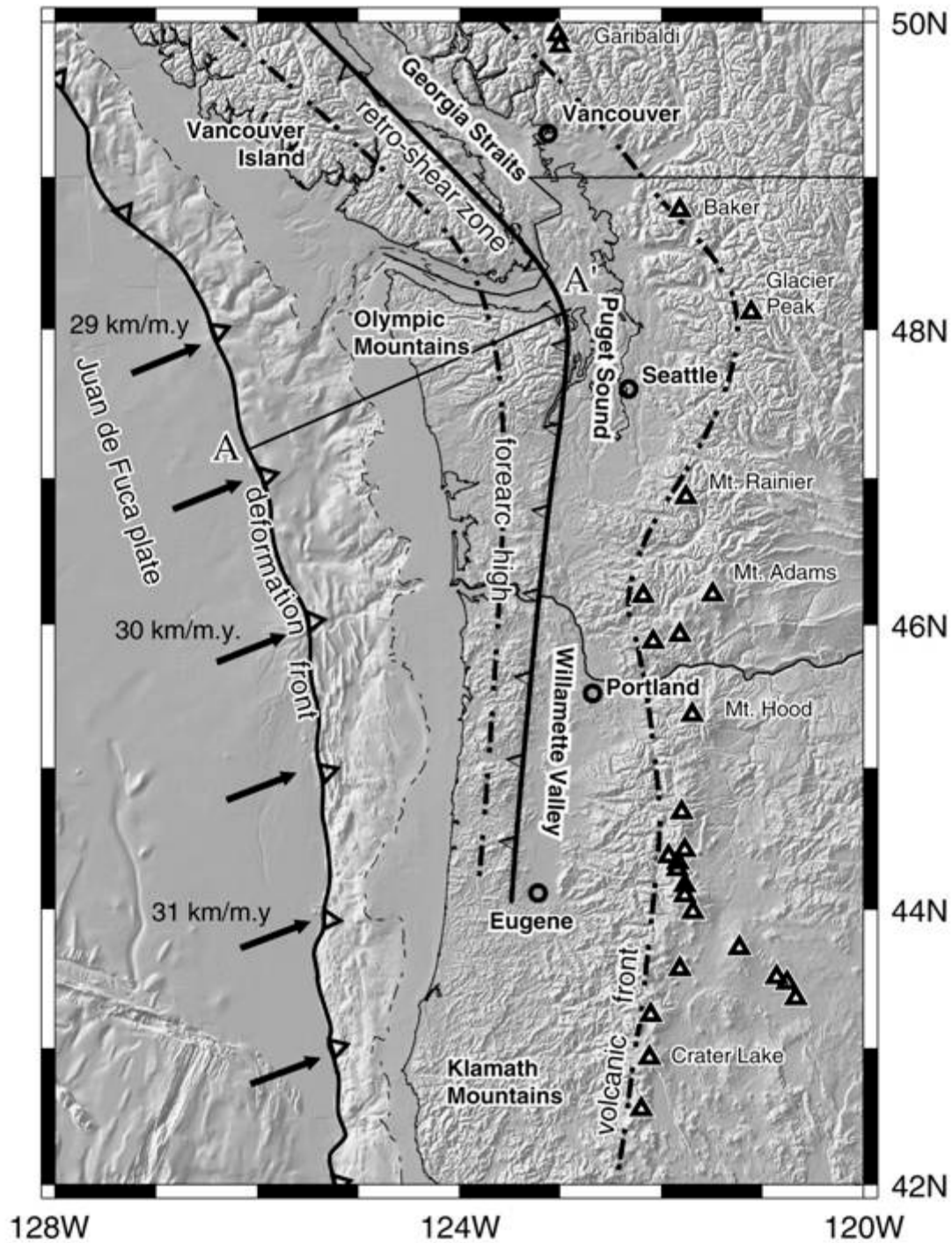
Sense and magnitude of vertical axis rotation similar
Slide from Rick Allmendinger, 2007

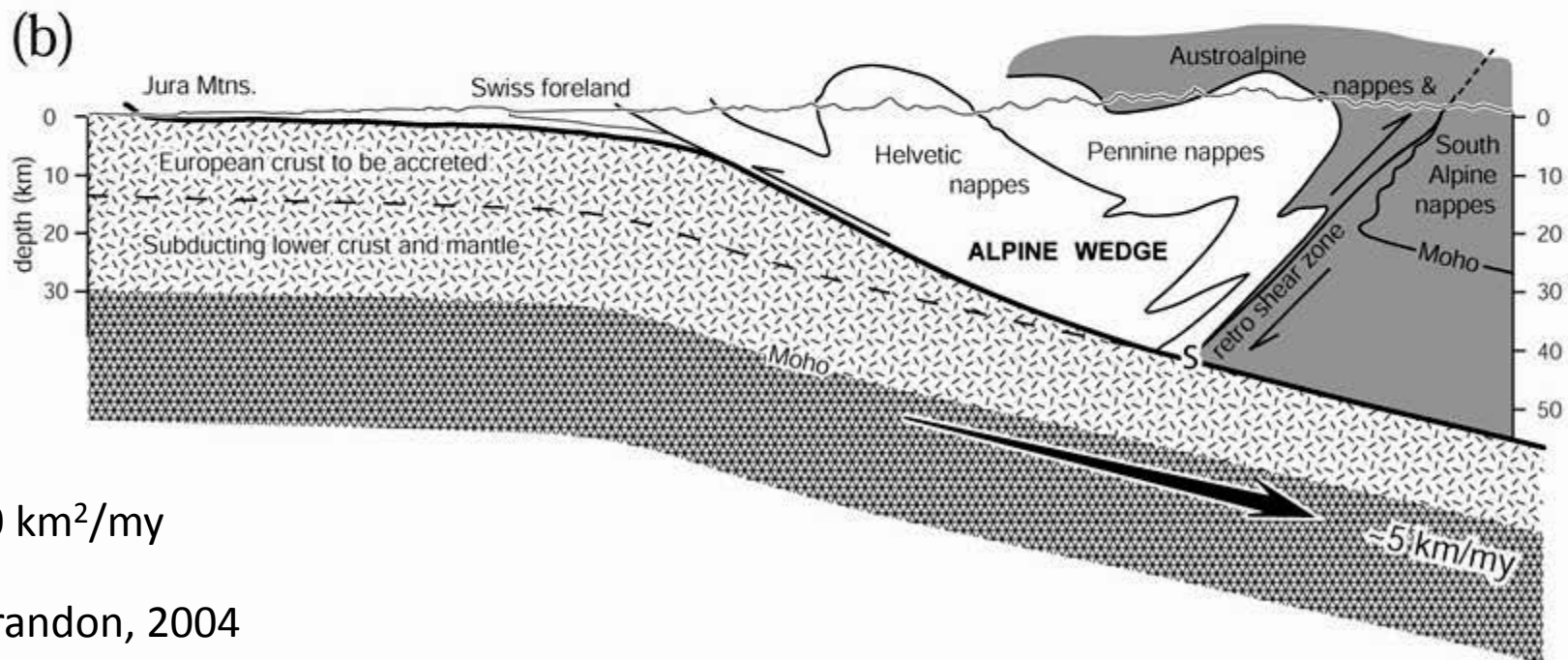
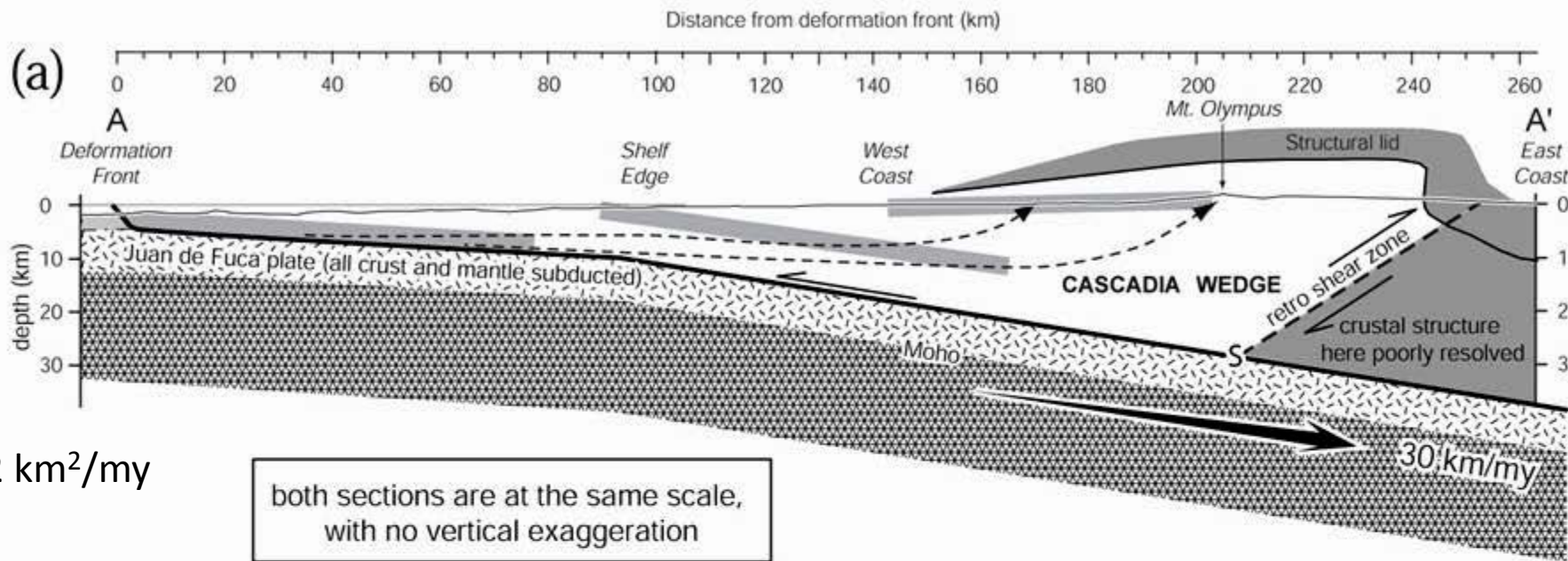
Concept of a Double-Sided Wedge



Sandbox experiment of Malavieille (1984), producing a double-side wedge.
Figure: Brandon, 2004

Brandon, 2004





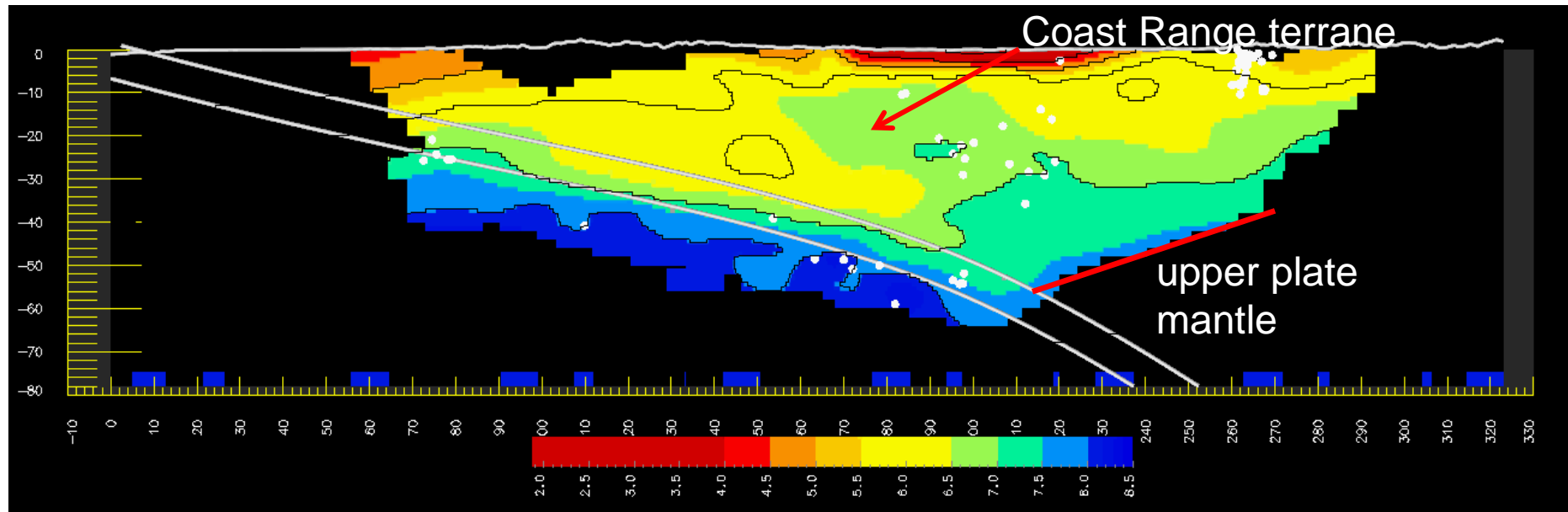
$$Fa = 52 \text{ km}^2/\text{my}$$

$$Fa = 60 \text{ km}^2/\text{my}$$

Brandon, 2004

Olympic Mtns.

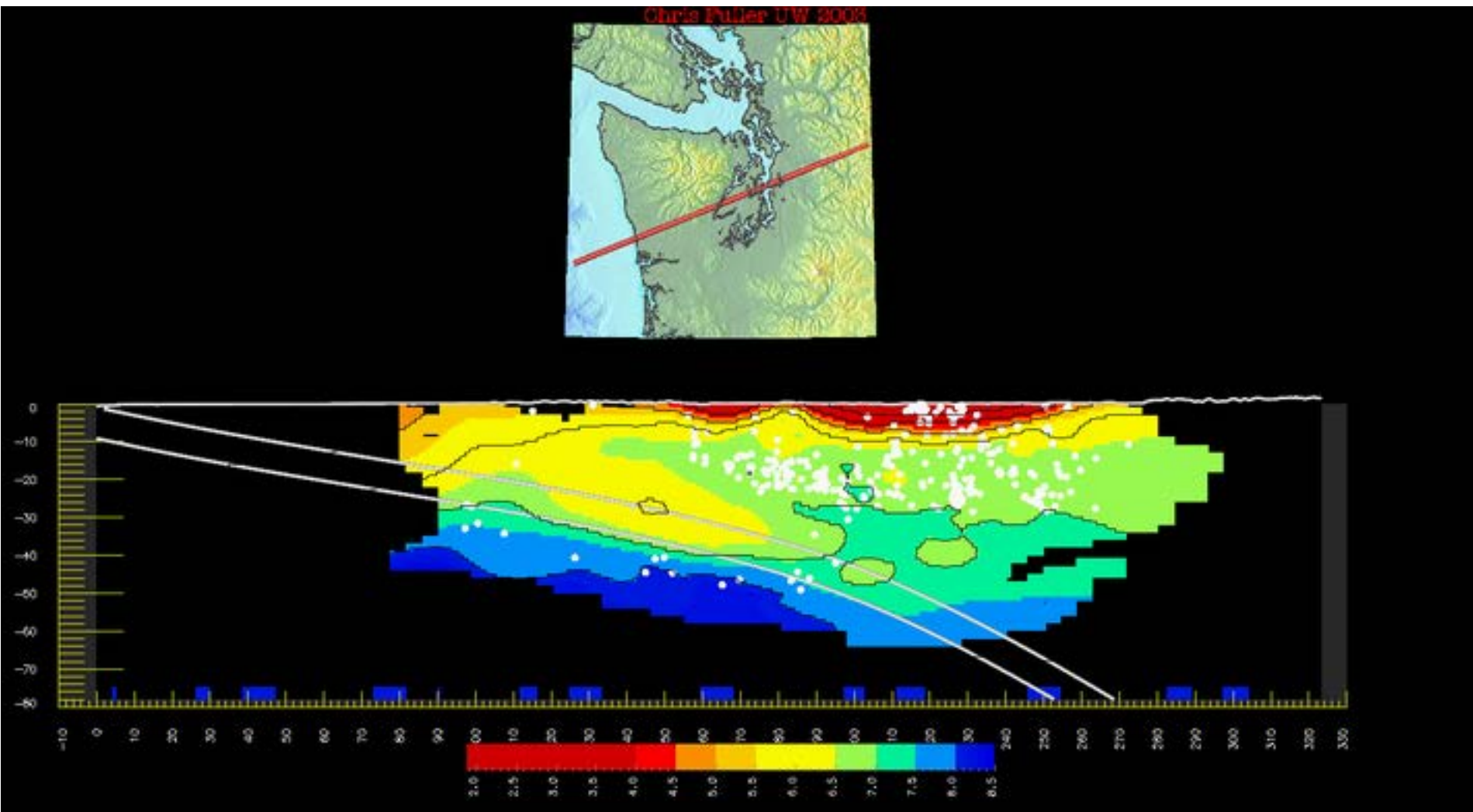
Puget Sound



The velocity tomography of Preston and Creager (2003) show that sedimentary rocks extend back beneath Coast Range lid, and that the upper plate Moho intersects the subducting plate beneath Puget Sound, ~40 km rearward of the rear of the wedge.

There is no “lithologic” backstop to localize wedge deformation!





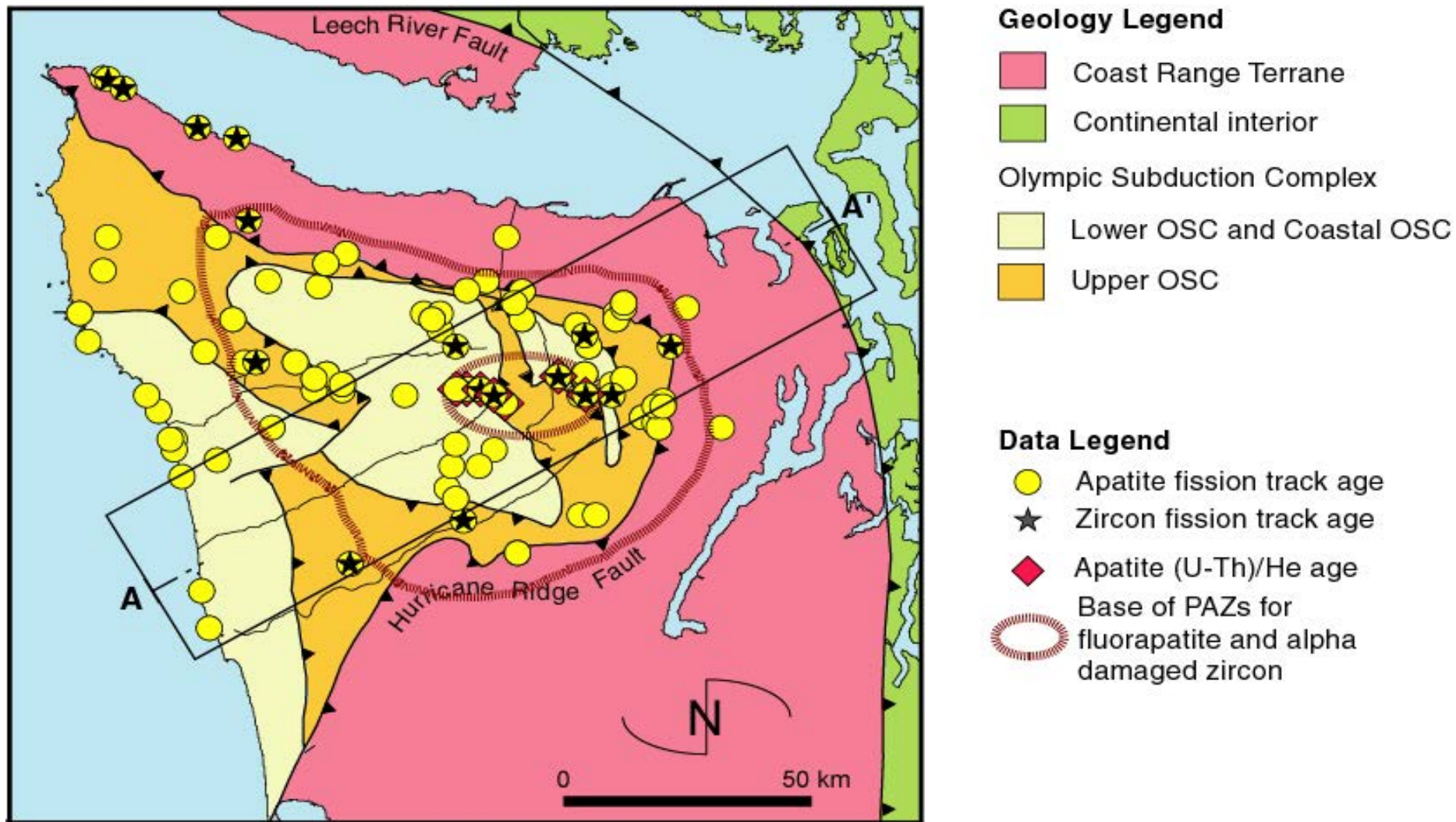
Movie from Chris Fuller, using data from Preston and Creager (2003)

Early Miocene turbidites of the Lower OSC, Presently Exposed on Mt. Olympus. Accreted from the front of the wedge.

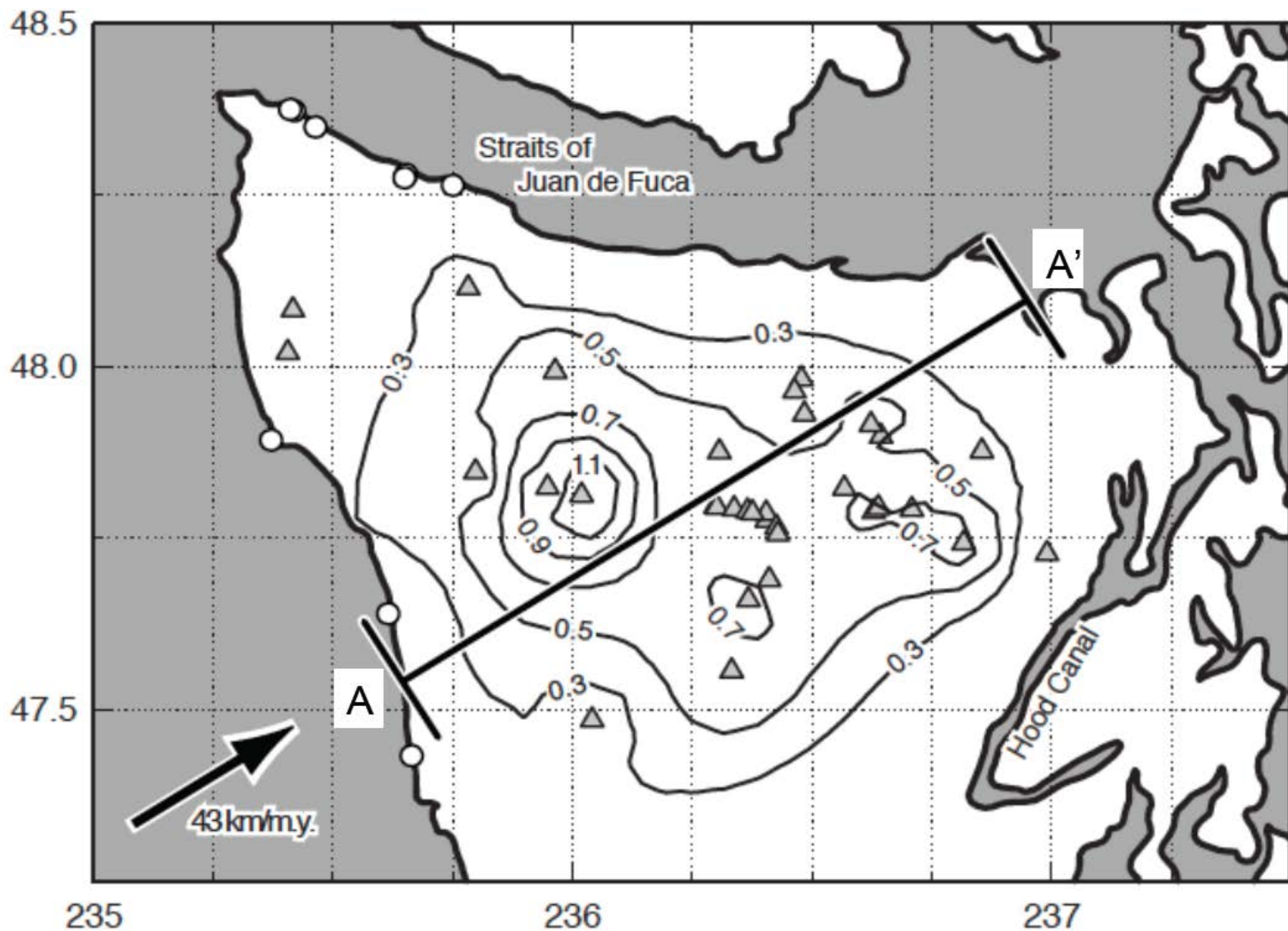


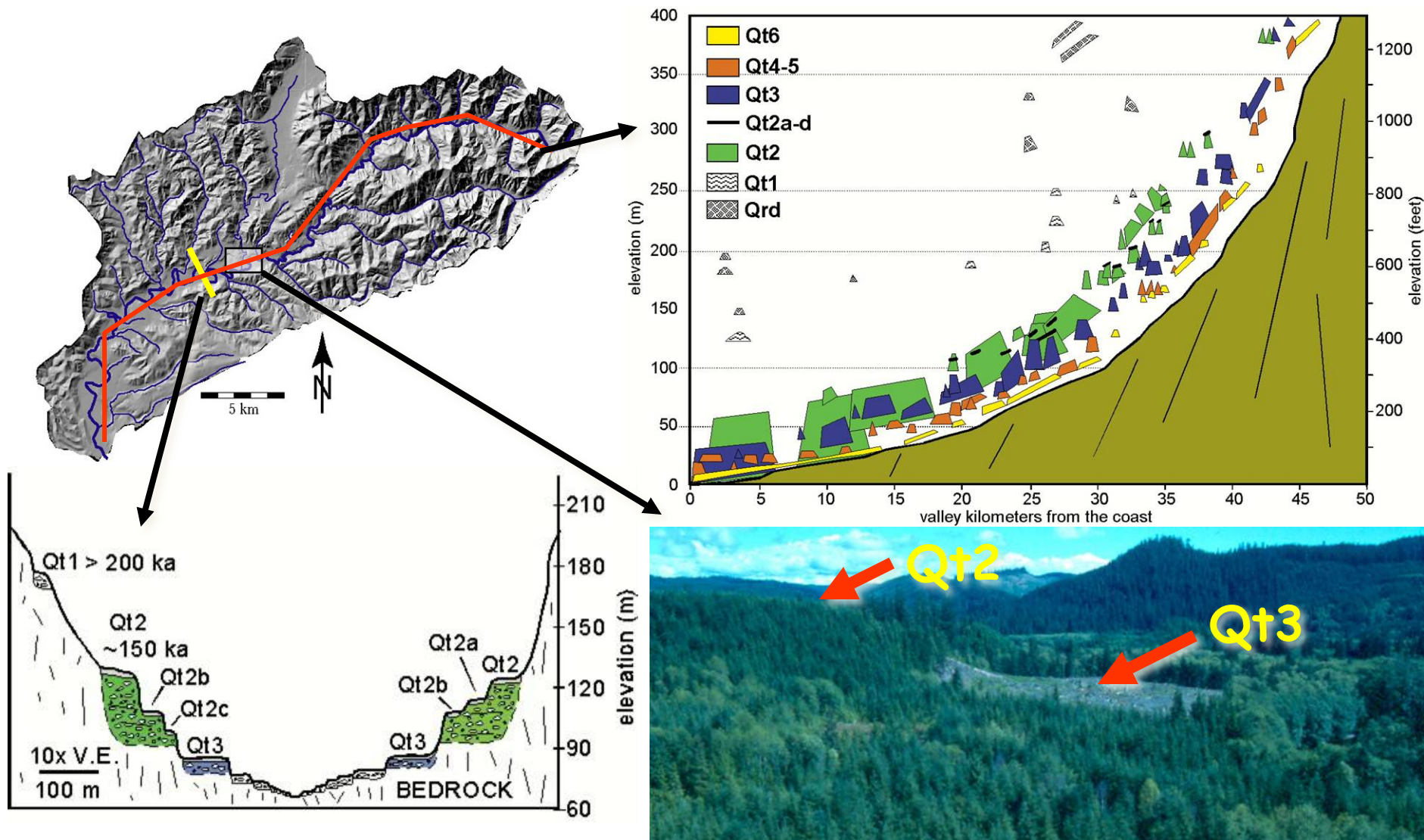
Picture: Mark Brandon

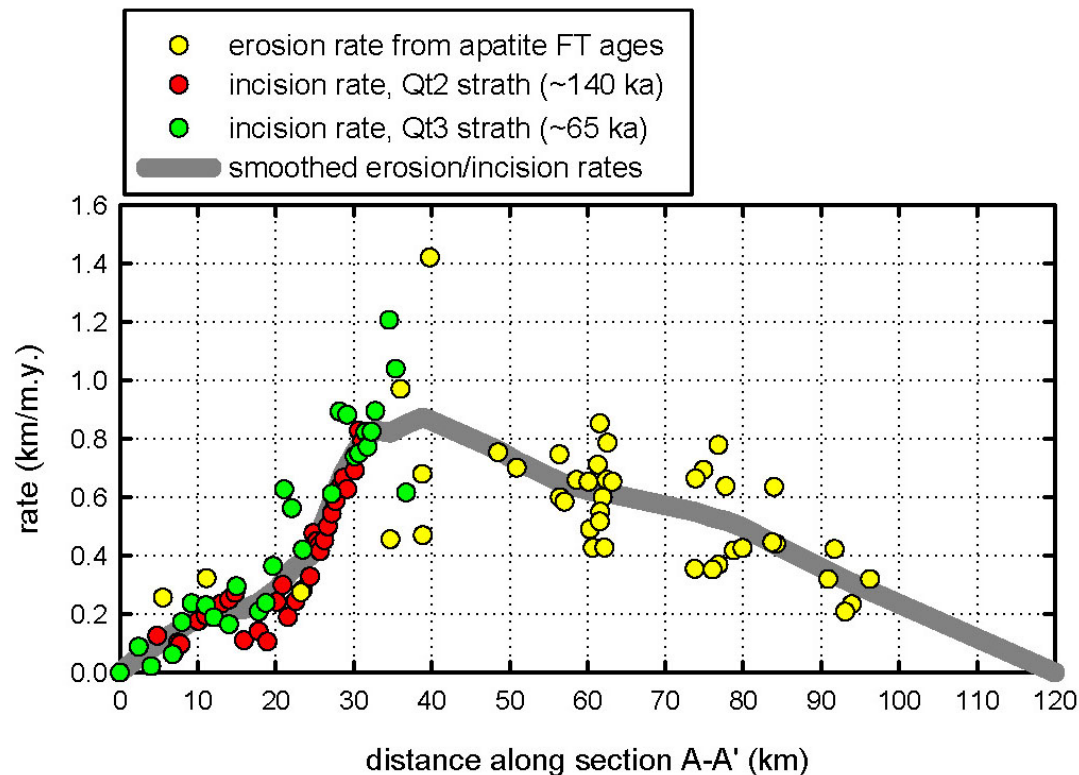
Thermochronometric Evidence for a Steady State Balance between Accretionary and Erosional Fluxes



Batt et al., 2001, JGR

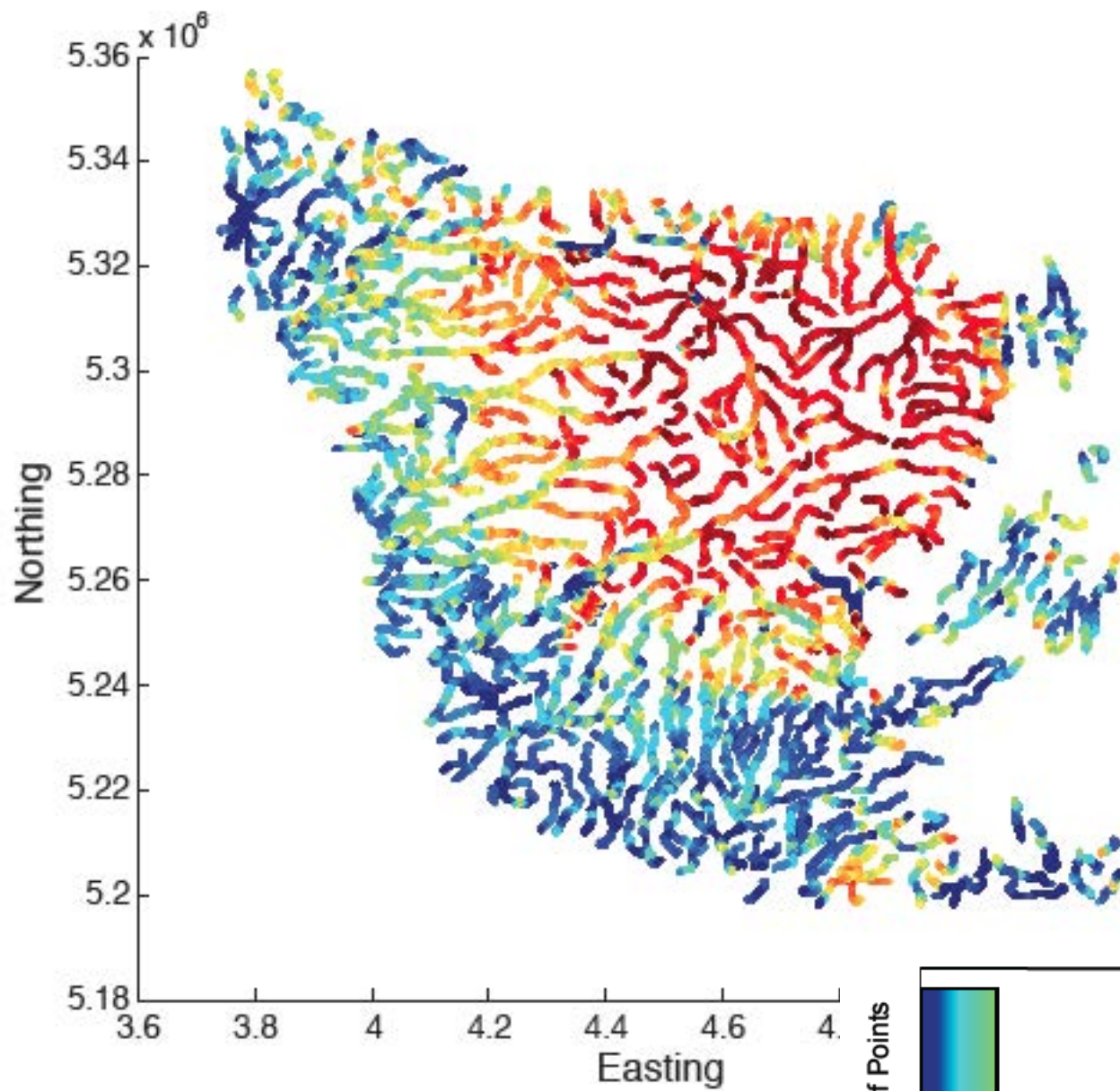




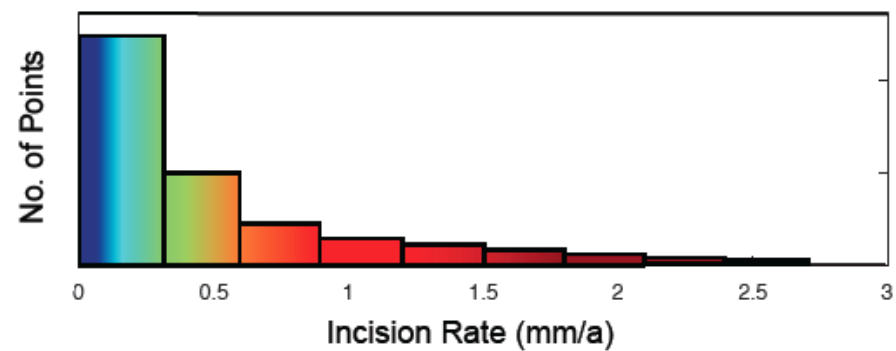


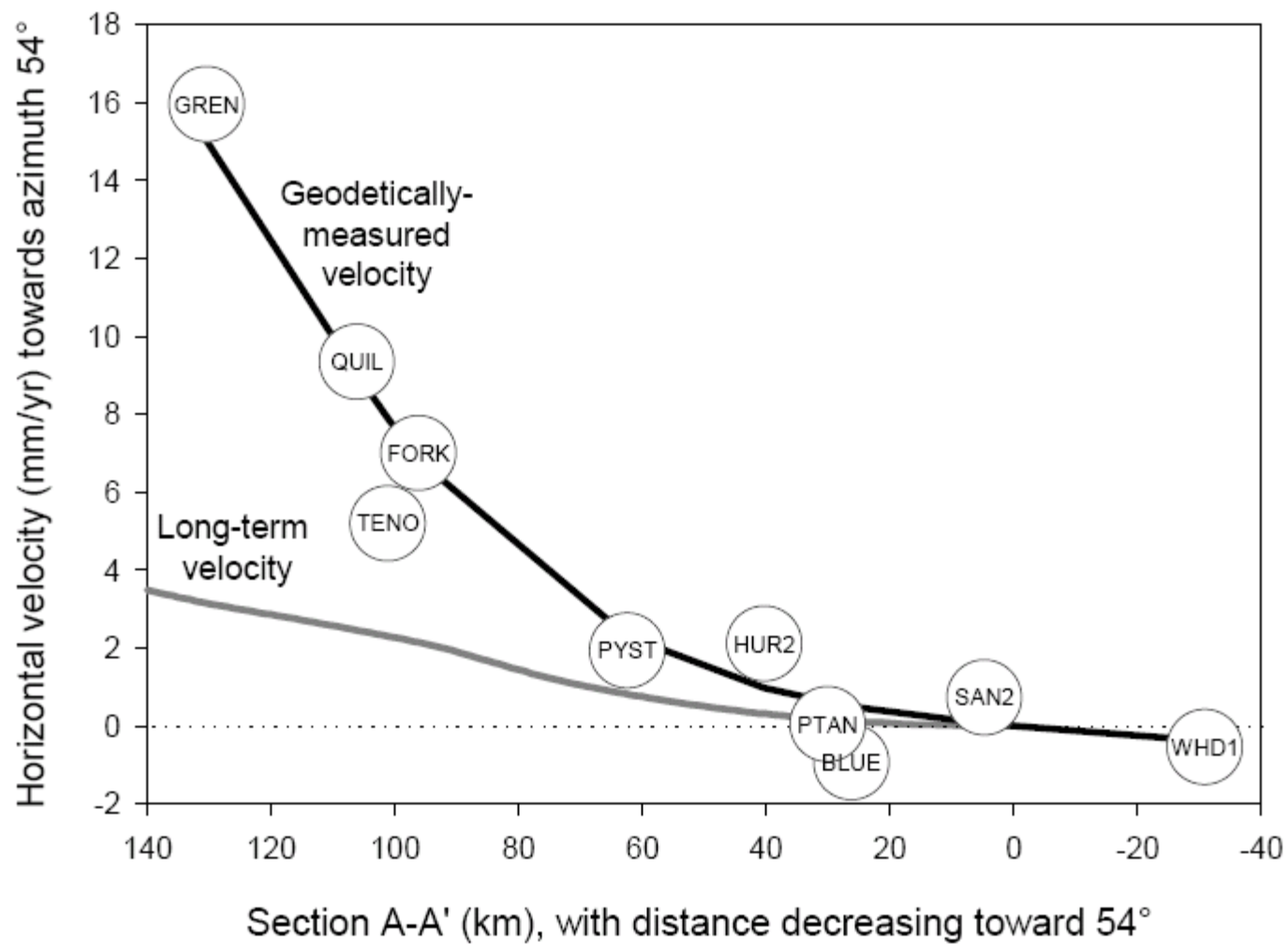
Strath Uplift Rates and FTA Erosion Rates

- FTA erosion rates compare closely with strata uplift rates, indicating that erosion is equal to uplift.
- The long-term erosional flux out of section A-A' is $57 \text{ km}^2 / \text{m.y.}$, which compares closely with the present accretionary flux of $52 \text{ km}^2 / \text{m.y.}$
- Error bars are at the 95% confidence limit for FTA erosion rates and strath uplift rates.

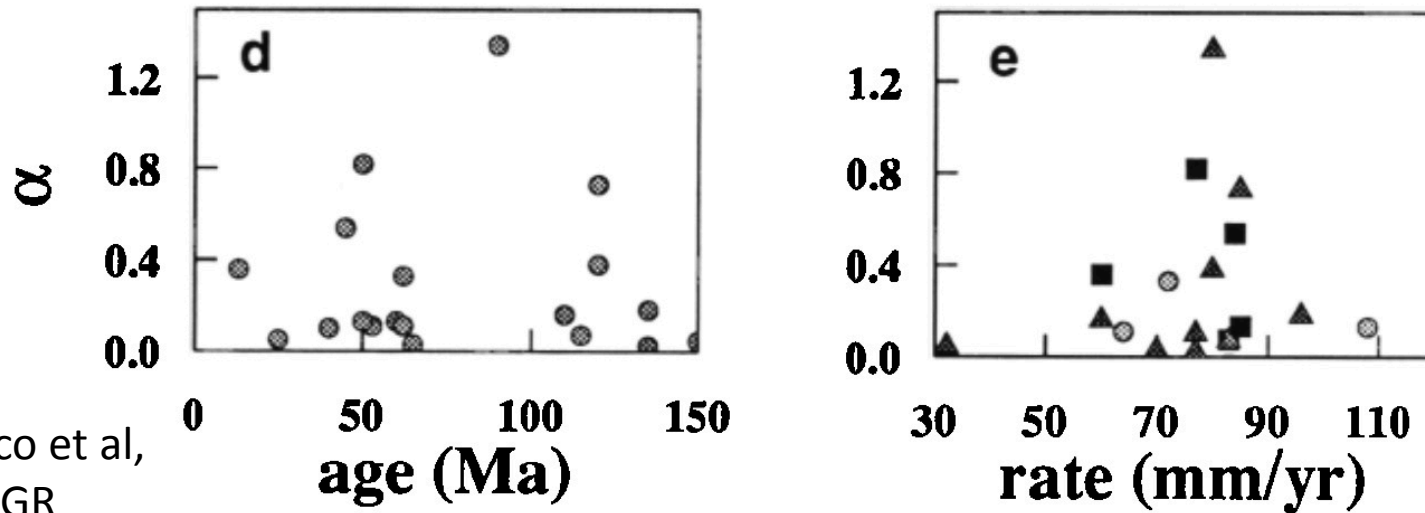


Elizabeth Brown and Mark Brandon, work
in progress





Seismic Coupling (α) as a function of the Age of the Subducting Plate and Rate of Subduction

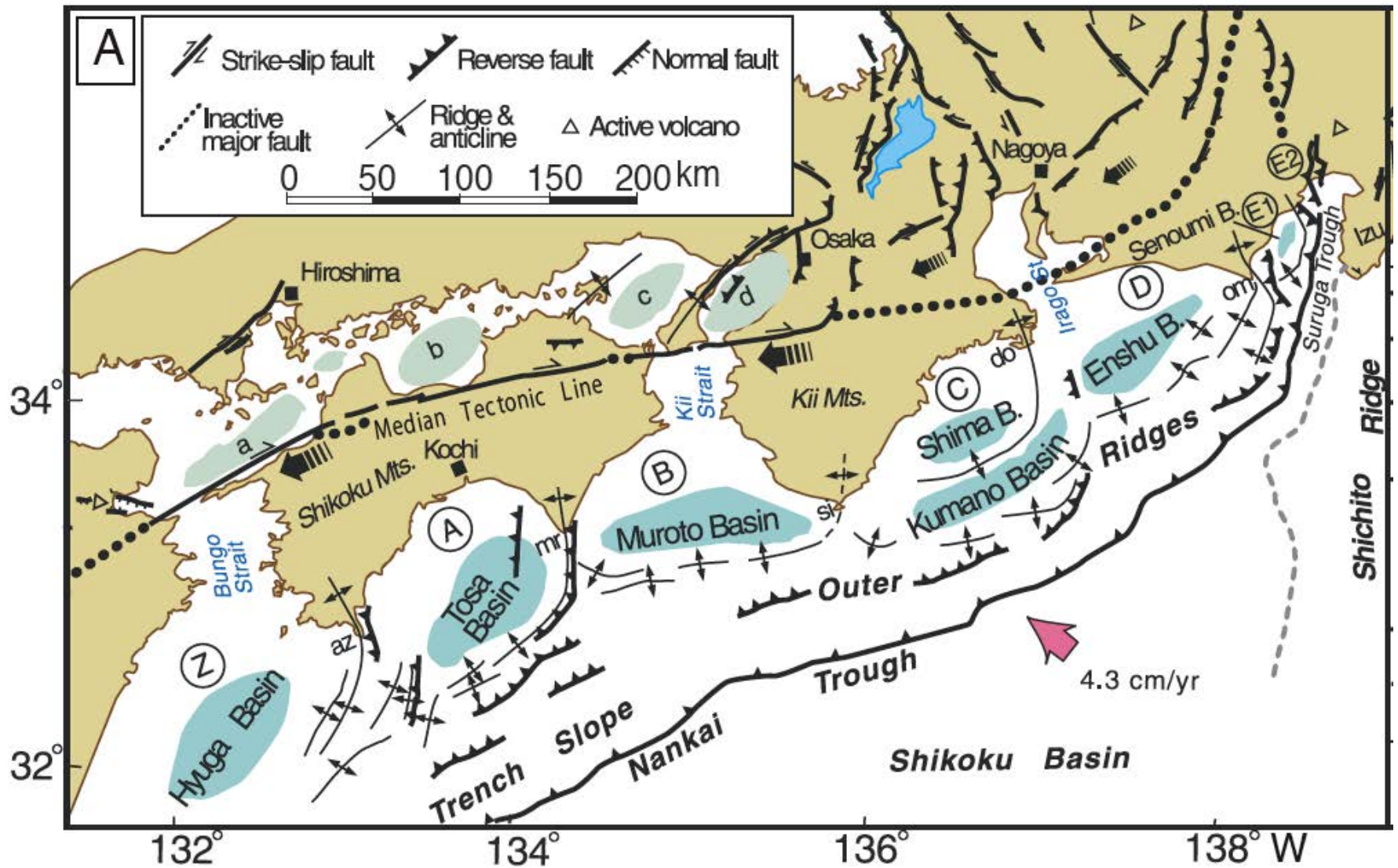


Pacheco et al,
1993 JGR

Fig. 11. Downdip width (W) as a function of (a) age of the ocean floor being subducted and (b) plate rate. Squares represent subduction zones with upper plates approaching the axis of the trench in the hotspot reference frame, triangles for upper plates retreating from the trench and circles for plates with mostly transverse motion. Seismic coupling coefficient α as a function of (c) downdip width W , (d) age of the ocean floor being subducted, and (e) relative plate rate; symbols same as in Figure 11b.

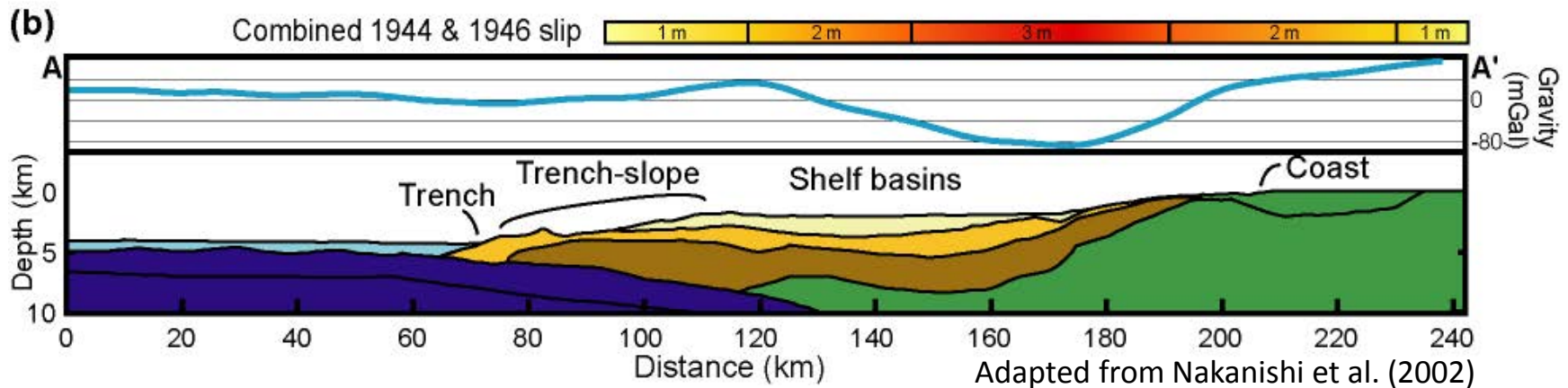
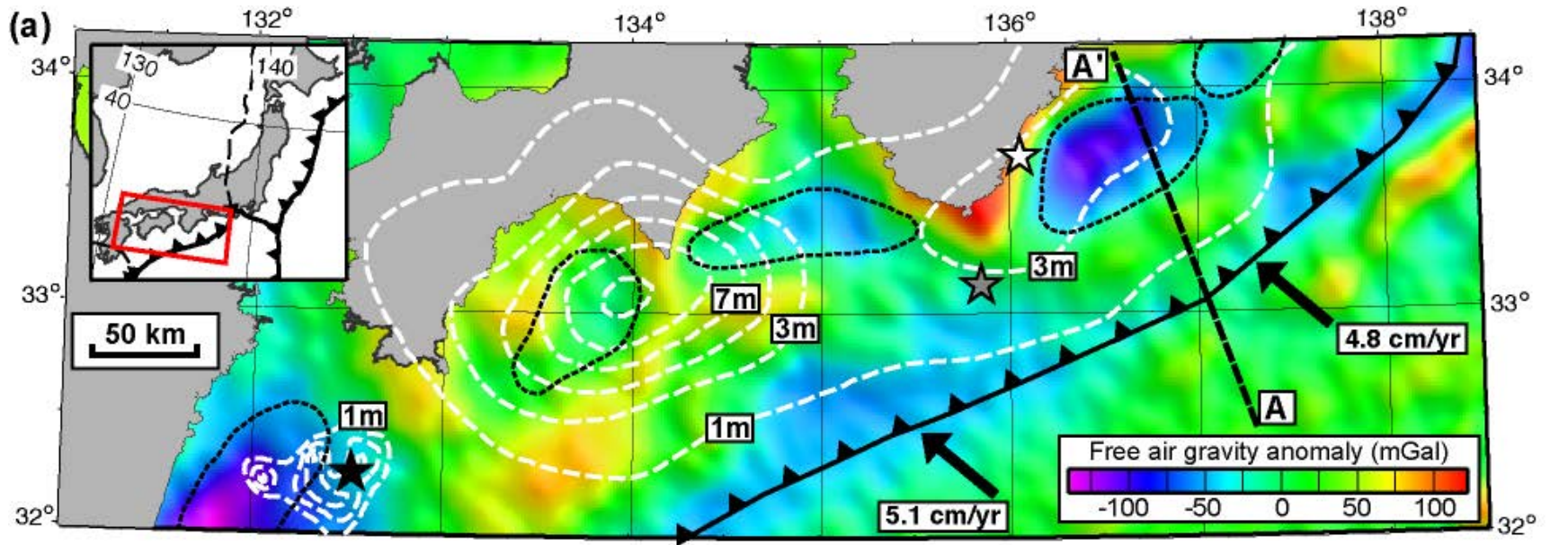
Seismic coupling is defined as the fraction of slip on the subduction zone that occurs during seismic events, relative to the total slip.

Nankai Margin

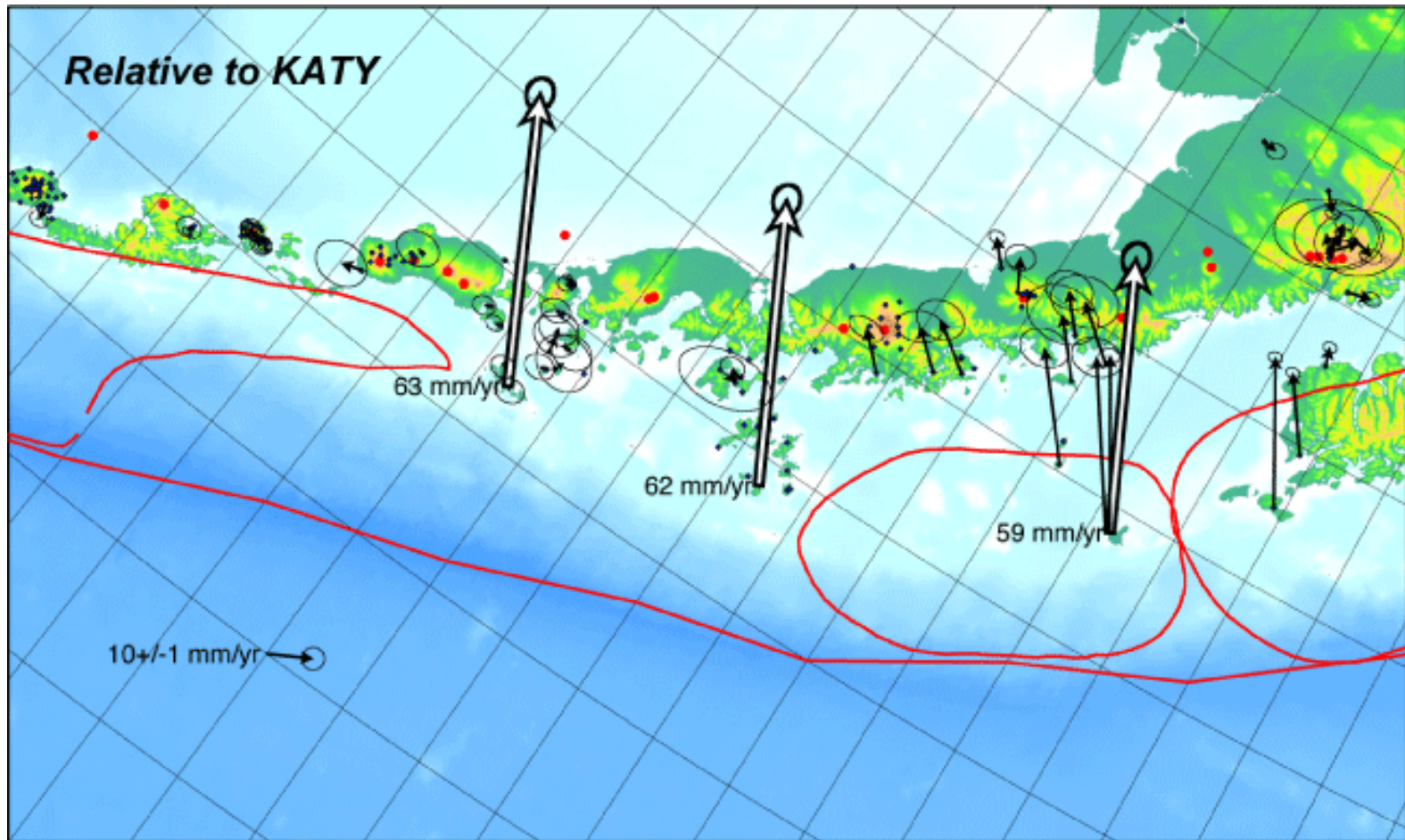


From: Wells et al., 2003

Nankai, SE Japan

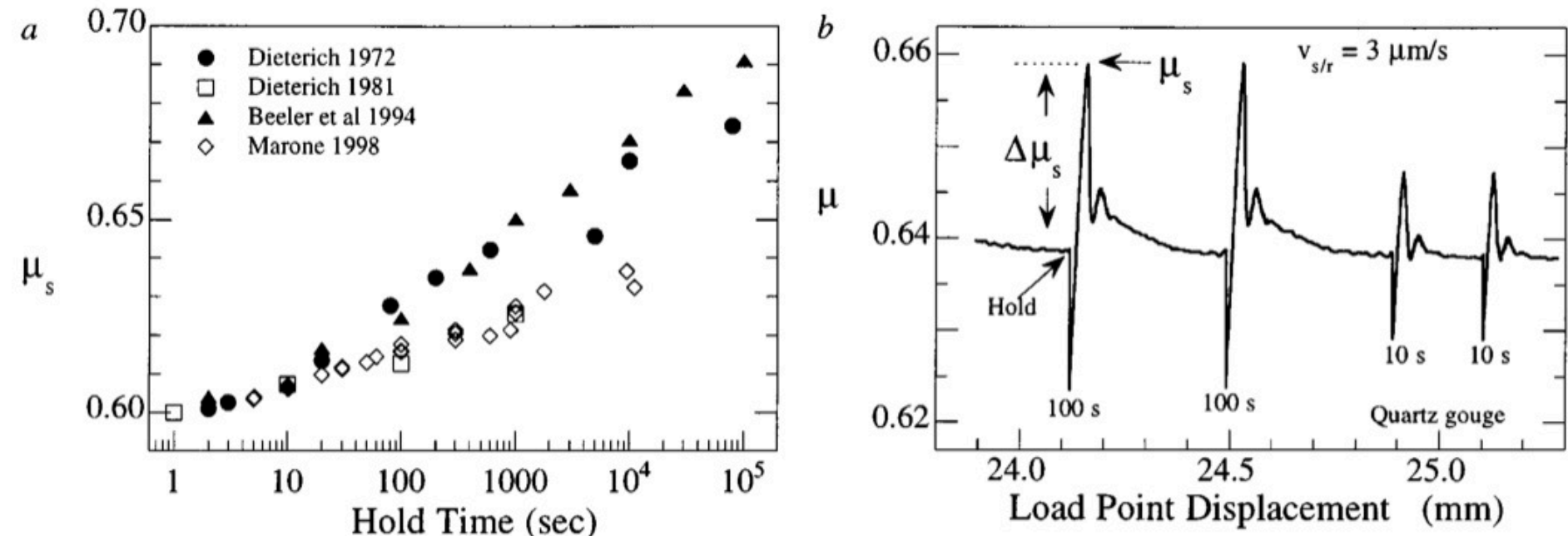


Fuller et al., 2006 Geology (also see Song and Simons, 2002, and Wells et al., 2003)



No geodetic coupling in Shumagin “seismic gap”, eastern Aleutians (figure and data from Jeff Freymueller and others, 2003)

Faulting Healing is the Fundamental Process Responsible for Seismic Slip



Results from hold tests for frictional behavior during sliding between two rock surfaces.
(Chris Marone, 1998, Annual Reviews)

μ_s = static friction coefficient (maximum shear stress/normal stress before slip).

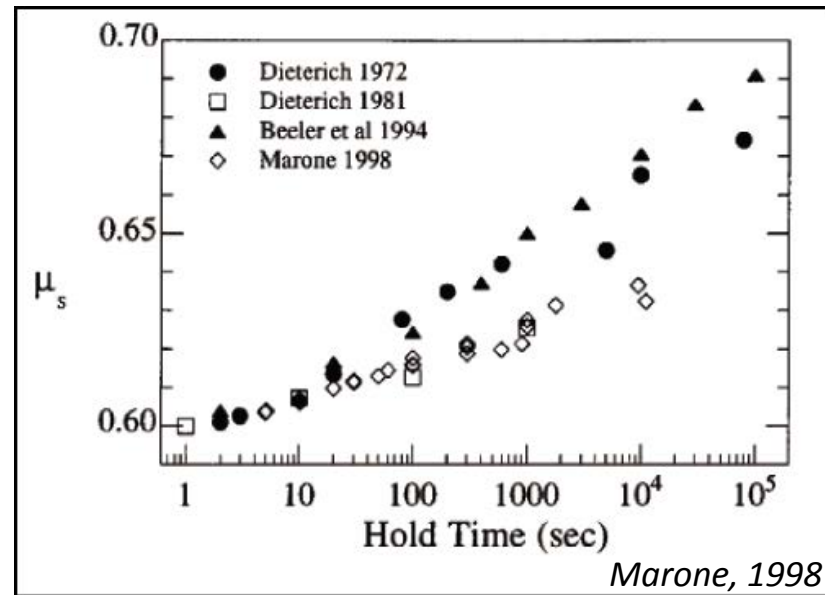
μ = Coulomb stress ratio = shear stress/normal stress.

hold time = amount of time that the sliding surfaces are held at rest before loading.

load point displacement = amount of sliding between the rock surfaces.

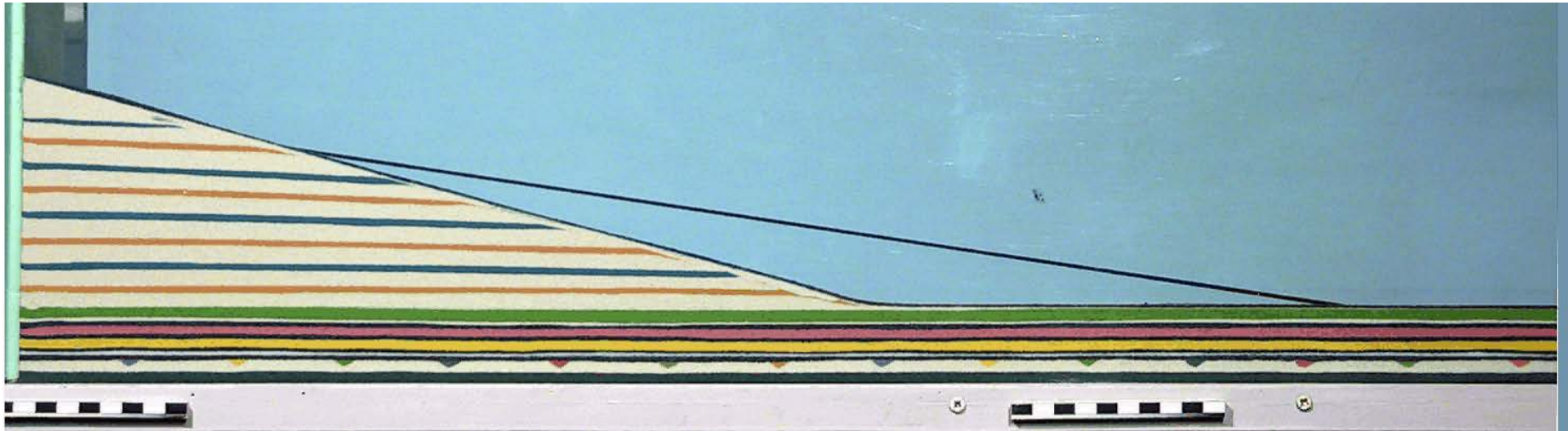
Linking Seismic Slip and Wedge Stability

Key factor: Variations in fault healing



- Longer intervals between plate interface slip leads to:
- (1) greater fault strength
- (2) increased stress drops during slip events
- (3) larger moment release during EQs

Accretion and Erosion in Wedge



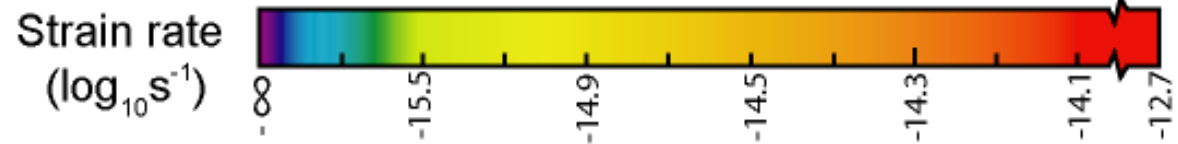
Wedge deformation is limited not by material strength of the overriding plate but rather by its integrated strength.

Movie from Konstantinovskaia and Malavieille, 2005 “G Cubed”

Frictional Model

$$\phi = 24^\circ$$

$$\phi_b = 8^\circ$$



Fuller et al., 2006



0.00

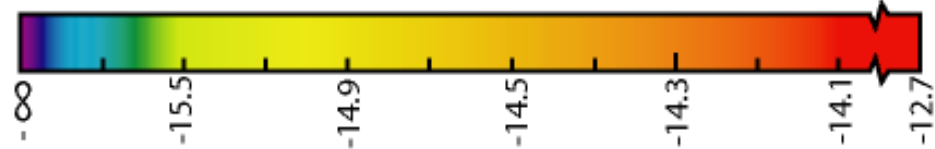


Frictional Model

$$\phi = 24^\circ$$

$$\phi_b = 8^\circ$$

Strain rate
($\log_{10} \text{s}^{-1}$)

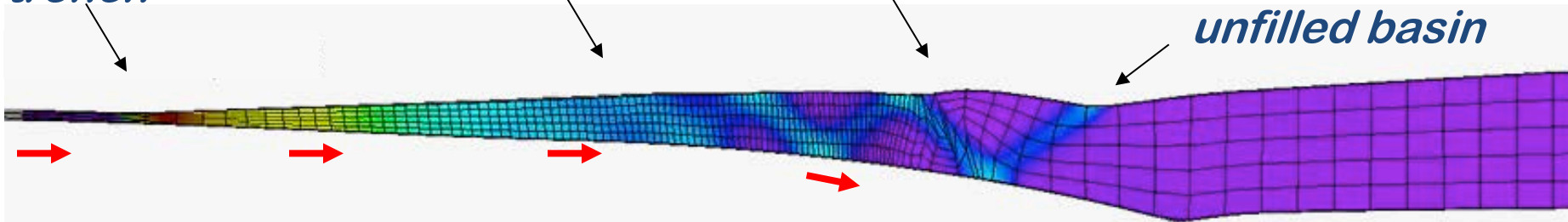


trench

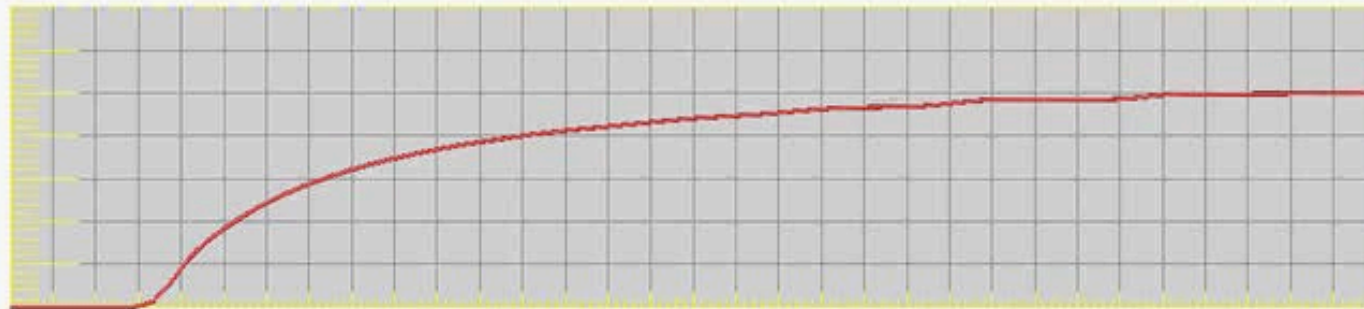
trench slope

surface rollover

unfilled basin



15.00



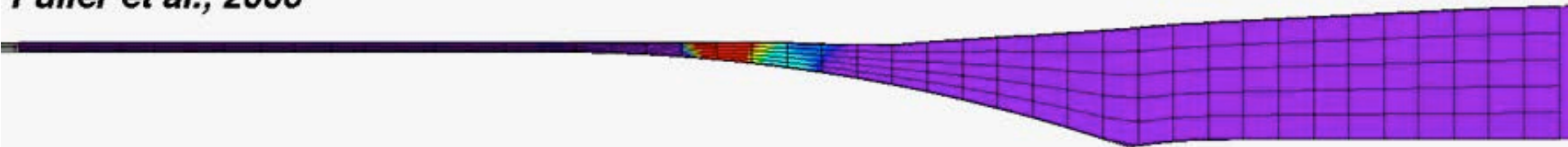
Frictional Model with Sedimentation

$$\phi = 24^\circ$$

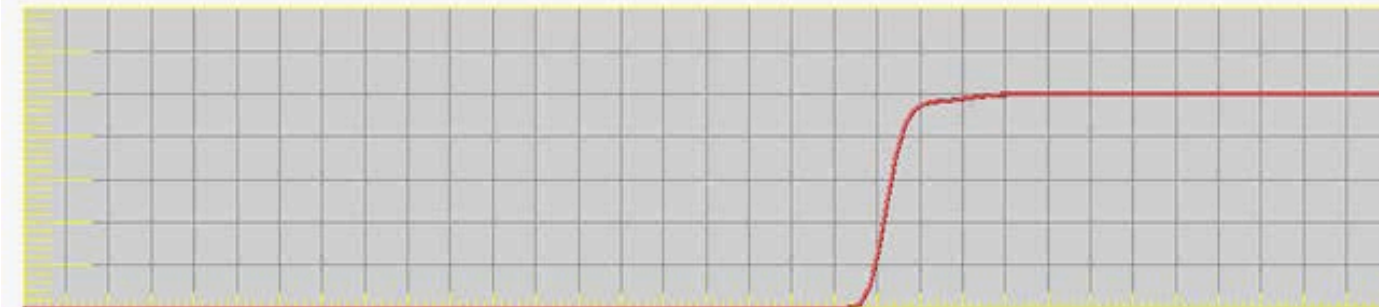
$$\phi_b = 8^\circ$$



Fuller et al., 2006

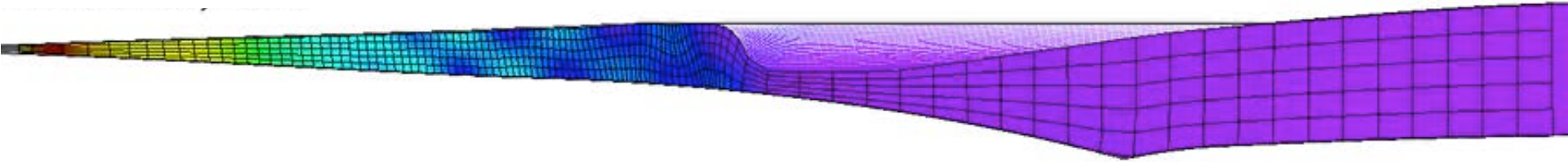


0.00

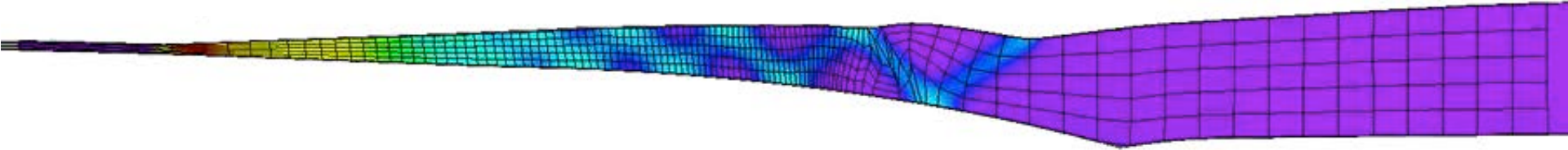


Effect of Sedimentation

non-deforming



deforming





Basins

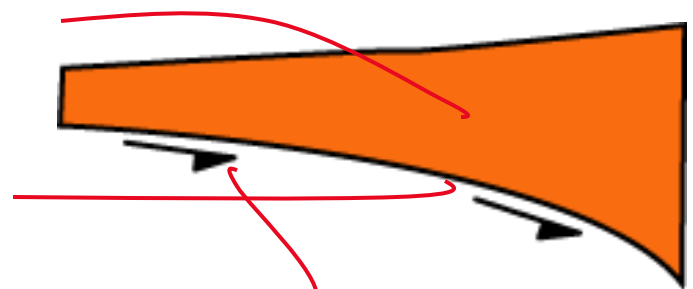


No Basins

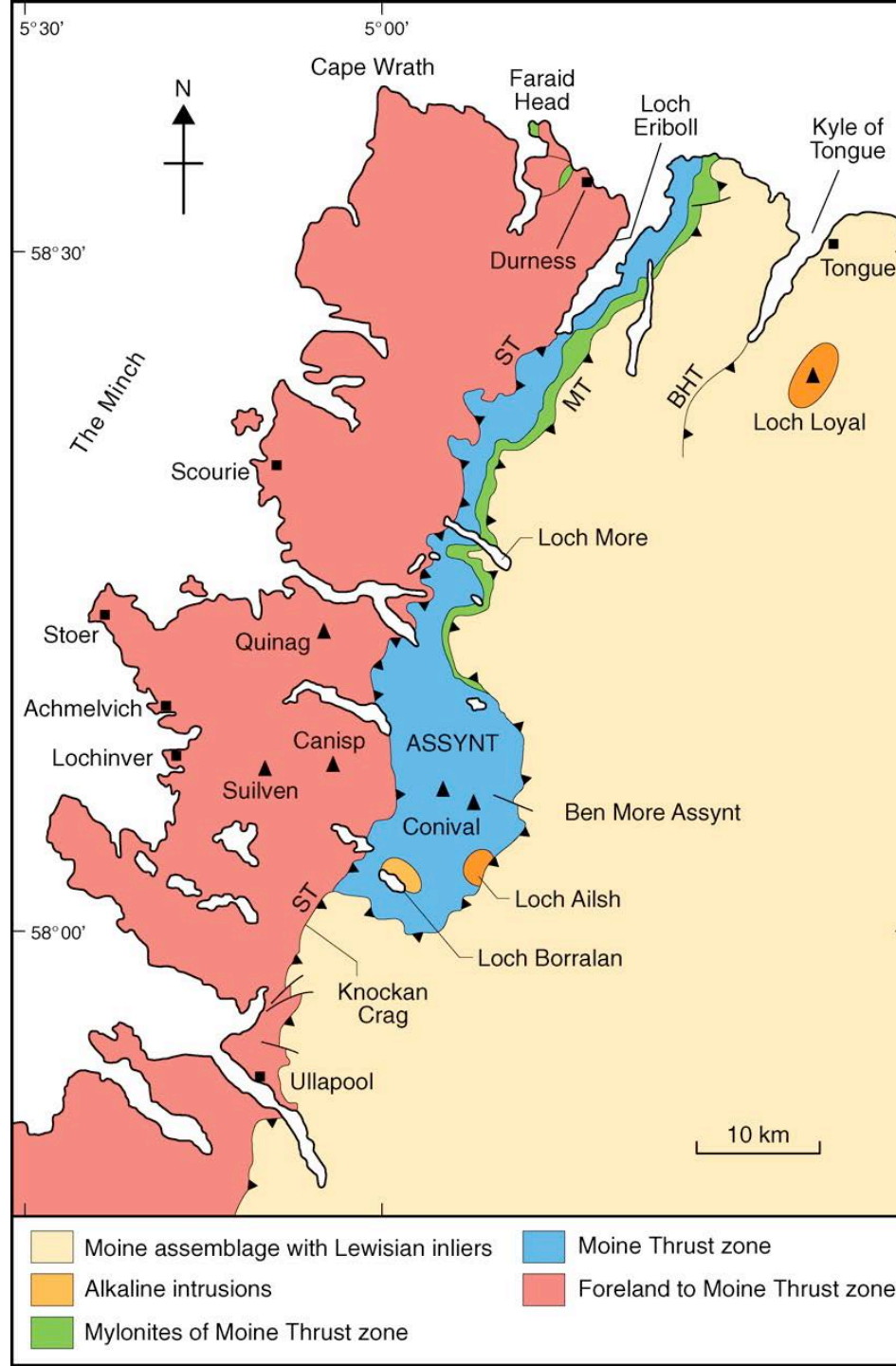


weaker wedge

shallower dip



stronger thrust



Searle et al, 2010